Cellular Physiology and Biochemistry

Cell Physiol Biochem 2026;60:427-444
DOI: 10.33594/000000881
Published online: 18 August 2026
Accepted: 31 July 2026

Published by Cell Physiol Biochem Press GmbH&Co. KG, Duesseldorf
www.cellphysiolbiochem.com

Original Paper

Hange-Shashin-to Suppresses Serotonin-Induced Neurogenic Intestinal Contraction via Inhibition of 5-HT3A Receptor Signaling

Kaori Sato-Numata[a] Ryo Takayama[b] Ayako Sakai[a] Tomohiro Numata[a]

[a]Department of Integrative Physiology, Graduate School of Medicine, Akita University, Akita 010-8543, Japan, [b]School of Medicine, Akita University, Akita 010-8543, Japan

Key Words
Acetylcholine release • Hange-shashin-to • Irritable bowel syndrome • Serotonergic signaling • 5-HT3 receptor

Abstract
Background/Aims: Hange-shashin-to (HST) is a standardized multi-component herbal formulation widely used for the treatment of irritable bowel syndrome (IBS), a functional gastrointestinal disorder characterized by dysregulated serotonergic signaling and abnormal intestinal motility. Despite its clinical application, the cellular mechanisms underlying its therapeutic effects remain unclear. This study investigated the effects of HST on serotonin (5-HT)-induced neuronal responses and the underlying role of 5-HT3A receptor signaling. ***Materials:*** Differentiated PC12 cells were used as a neuron-like model to evaluate 5-HT-induced cell shrinkage, membrane depolarization, intracellular Ca^{2+} elevation, and acetylcholine release. Whole-cell patch-clamp recordings were performed in HEK293T cells expressing 5-HT3A receptors to examine receptor-mediated cation currents. The effects of HST on 5-HT-induced colonic contractions were further evaluated using ex vivo rat colonic tissue. ***Results:*** HST attenuated 5-HT-induced cell shrinkage in a concentration-dependent manner and suppressed membrane depolarization, intracellular Ca^{2+} elevation, and acetylcholine release in PC12 cells. Patch-clamp analysis demonstrated that HST directly inhibited 5-HT3A receptor-mediated cation currents without altering voltage dependence or reversal potential. Furthermore, HST significantly reduced 5-HT-induced colonic contractions, with efficacy comparable to that of the selective 5-HT3 receptor antagonist ramosetron. ***Conclusion:*** HST suppresses 5-HT-induced neuronal excitation through inhibition of 5-HT3A receptor-mediated ion channel activity, resulting in reduced downstream intestinal motor responses. These findings identify the 5-HT3A receptor as a molecular target of HST and provide mechanistic insight into its pharmacological actions on 5-HT-mediated intestinal dysfunction.

K. Sato-Numata and R. Takayama contributed equally to this work.

Tomohiro Numata
Department of Integrative Physiology, Graduate School of Medicine, Akita University, Akita 010-8543, Japan
E-Mail: numata@med.akita-u.ac.jp
ORCID ID
Kaori Sato-Numata 0000-0002-9369-4261, Tomohiro Numata 0000-0002-5719-4884

Introduction

Irritable bowel syndrome (IBS) is a prevalent functional gastrointestinal disorder characterized by chronic abdominal pain, altered bowel habits, and abnormal intestinal motility. The pathophysiology of IBS is multifactorial, involving interactions among the central nervous system (CNS), hypothalamic–pituitary–adrenal (HPA) axis, enteric nervous system (ENS), and gut microbiota, collectively termed the gut–brain axis [1]. Dysregulation of this bidirectional network contributes to visceral hypersensitivity and impaired intestinal function in IBS [1-3]. Serotonin (5-hydroxytryptamine, 5-HT) is a key mediator of gastrointestinal function, regulating secretion, motility, and visceral sensitivity [1, 4, 5]. 5-HT plays a central role in gastrointestinal motility, secretion, and sensory signaling within the gut–brain axis [6]. More than 95% of the body's 5-HT is localized in the gastrointestinal tract, where it serves as a major neurotransmitter in the ENS [7]. Among the 5-HT receptor subtypes, the 5-HT3 receptor is a ligand-gated ion channel that plays a central role in excitatory neurotransmission and is implicated in IBS symptoms, particularly abdominal pain and diarrhea [4, 8, 9]. Accordingly, selective 5-HT3 receptor antagonists such as ramosetron are clinically used for diarrhea-predominant IBS (IBS-D) [8-10].

Hange-shashin-to (HST) is a traditional Japanese Kampo medicine composed of seven herbal ingredients, including *Pinellia tuber*, *Scutellaria root*, *Processed Ginger*, *Glycyrrhiza*, *Jujube*, *Ginseng*, and *Coptis rhizome.* It is widely prescribed for gastrointestinal disorders such as diarrhea, nausea, and IBS [11]. Recent studies suggest that components of HST can modulate ion channels and neuronal signaling pathways. For instance, HST has been reported to alleviate pain by inhibiting sodium channels [12], and to improve symptoms in patients with IBS-D and chemotherapy-induced diarrhea [13, 14]. However, its direct effects on serotonergic signaling and enteric neurotransmission remain insufficiently characterized.

Changes in cell volume are closely linked to transmembrane ion transport and reflect fundamental cellular processes such as excitation and secretion [15-19]. In neuronal systems, excitatory stimuli are associated with transient cell swelling due to cation influx, whereas secretagogue stimulation induces a sustained reduction in cell volume, termed secretory volume decrease (SVD), which is coupled to neurotransmitter release [20]. Therefore, analysis of 5-HT-induced volume changes provides insight into the ionic mechanisms underlying neurotransmission.

In this study, we used PC12 cells treated with nerve growth factor (NGF) as a model for nerve cells. We examined how these cells react to 5-HT and how HST influences them. Our results show that HST prevents the reduction in cell volume caused by 5-HT and blocks related processes, such as changes in membrane current, depolarization, intracellular Ca^{2+} entry, acetylcholine release, and intestinal contractility. These findings suggest that inhibition of 5-HT3A receptor-mediated signaling represents a key mechanism underlying the therapeutic effects of HST in IBS.

Materials and Methods

Cell culture, differentiation, and overexpression of 5-HT3A receptor

PC12 cells, derived from rat pheochromocytoma, were cultured in Dulbecco's Modified Eagle Medium (DMEM) supplemented with 5% fetal bovine serum, 5% horse serum, 30 units/mL penicillin, and 30 µg/mL streptomycin at 37°C in a humidified incubator with 5% CO_2. To induce differentiation toward a neuron-like phenotype, the cells were seeded at a density of 4×10^4 cells/well onto a 3.5-cm collagen-coated dish and cultured for 4 d in DMEM supplemented with 5% FBS, GlutaMAX (1×), and NGF (50 ng/mL), without horse serum. HEK293T cells were maintained in DMEM supplemented with 10% fetal bovine serum, 30 units/mL penicillin, and 30 µg/mL streptomycin. For receptor expression studies, HEK293T cells were transiently transfected with a plasmid encoding the human 5-HT3A receptor cloned into pIRES2-AcGFP1 (Takara Bio, Shiga, Japan) using Lipofectamine 2000 (Invitrogen, Carlsbad, CA, USA) following the manufacturer's

protocol. The human 5-HT3A receptor cDNA was obtained from the Genome Network Project clone and provided by the RIKEN BioResource Research Center (BRC) through the National BioResource Project of MEXT, Japan [21-24].

Reagents

Dimethyl sulfoxide (DMSO) was purchased from Wako Pure Chemical Industries Ltd. (Osaka, Japan). 5-HT (5-hydroxytryptamine), nifedipine, TTA-P2, ramosetron, and RS-127445 were obtained from Sigma-Aldrich (St. Louis, MO, USA) and Tocris (Bristol, UK). Hange-shashin-to (TJ-14), a clinically approved Kampo formulation, was obtained from Tsumura & Co. (Tokyo, Japan). TJ-14 is a standardized Kampo formulation composed of seven crude drugs as described in Kampo databases [25, 26]. The botanical and phytochemical characteristics of TJ-14 are summarized in Supplementary Table S1, and a representative manufacturer-provided 3D-HPLC fingerprint is shown in Supplementary Fig. S1. Hange-shashin-to powder was dissolved in DMSO at a concentration of 400 mg/mL for same-day use. HST stock solutions were prepared with a final concentration of DMSO in all experimental conditions of ≤0.1% (v/v). Vehicle controls were matched to the corresponding DMSO concentration. All other chemical reagents were purchased from commercial suppliers.

Animals

The animal experimental protocol was approved by the Akita University Animal Ethics Committee (Akita, Japan, Ethics Review Number: b-1-0408). Male Wistar rats, 8-12 weeks of age, were housed in a controlled environment at 22-25°C with a 12-h light/dark cycle and had free access to water and commercial diet.

Mean cell size measurements

Changes in cell size at room temperature were visualized using a microscope equipped with a low-light camera (ORCA-ER-1394, Hamamatsu Photonics, Shizuoka, Japan), and images were recorded with AquaCosmos software (version 2.0: Hamamatsu Photonics). Cell size in PC12 cells was quantified by measuring the cross-sectional area (CSA) of the cell body using ImageJ (NIH, Bethesda, MD, USA) [27]. This approach has been widely used as an established method for estimating relative changes in cell volume from two-dimensional imaging [28]. PC12 cells were exposed to serotonin (5-HT; 50 μM) or high extracellular potassium (High K^+; 80 mM), with or without extracellular Ca^{2+}, Hange-shashin-to (HST), ramosetron, or TTA-P2, or High K^+ Tyrode's solution. Tyrode solution contained (in mM): 140 NaCl, 5 KCl, 1 $MgCl_2$, 2 $CaCl_2$, 10 D-glucose, and 10 HEPES (pH 7.4 adjusted by NaOH, and 330 mosmol/kg-H_2O adjusted by D-mannitol). High K^+ Tyrode's solution contained (in mM): 65 NaCl, 80 KCl, 1 $MgCl_2$, 2 $CaCl_2$, 10 D-glucose, and 10 HEPES (pH 7.4 adjusted by NaOH, and 330 mosmol/kg-H_2O adjusted by D-mannitol). To observe the effects of Ca^{2+} chelation, we preincubated cells with a Ca^{2+}-free Tyrode's solution containing (in mM): 140 NaCl, 5 KCl, 1 $MgCl_2$, 10 EGTA, 10 D-glucose, and 10 HEPES (pH 7.4 adjusted by NaOH, and 330 mosmol/kg-H_2O adjusted by D-mannitol) in the presence of 50 μM BAPTA-AM for 60 min, and then we performed experiments by applying a Ca^{2+}-free Tyrode's solution. Changes in the cell area attached to the coverslip were assessed over a 30-min period after a 45-min preincubation with Tyrode's solution. The relative change in area was calculated as a percentage, using the stable baseline area measured at zero min of observation in Tyrode's solution prior to any experimental treatment. Tyrode's solution was used as the recording medium for all experiments.

Electrophysiology

Whole-cell patch-clamp recordings were performed in differentiated PC12 cells and HEK293T cells expressing the 5-HT3A receptor. HEK293T cells were mechanically dispersed by pipetting and fixed on glass coverslips. PC12 cells were plated onto collagen-coated glass coverslips. Membrane potentials and membrane currents in these cells were recorded at room temperature (22-25°C) by patch-clamp whole-cell recordings or nystatin-perforated whole-cell recordings with an Axopatch 200B (Axon Instruments/Molecular Devices, Union City, CA, USA). Patch electrodes prepared from borosilicate glass capillaries had an input resistance of 3-5 MΩ when filled with solution. Current signals were filtered at 5 kHz using a four-pole Bessel filter, digitized at 20 kHz, and recorded on a desktop computer. pCLAMP (version 10.5.1.0, Axon Instruments/Molecular Devices) software was used for command pulse control, and for data acquisition and

analysis. Data were also analyzed using Origin (OriginLab Corp., Northampton, MA, USA) software. Series resistance was compensated to minimize voltage errors (70-80%). The external solution contained (in mM) 120 NaCl, 5 KCl, 0.25 $CaCl_2$, 0.25 $MgSO_4$, and 10 HEPES (pH 7.4 adjusted by NaOH, and 300 mosmol/kg-H_2O adjusted by D-mannitol). The pipette solution contained (in mM) 100 NMDG-gluconate, 20 NMDG-Cl, 4 NaCl, 0.5 $CaCl_2$, 2 $MgSO_4$, 5 EGTA, 10 HEPES, and 2 Na_2ATP, 0.3 GTP-Na salt (adjusted to pH 7.3 with NMDG and to an osmolarity of 285 mosmol/kg-H_2O with D-mannitol). Resting membrane potential measurements were made using the nystatin-perforated whole-cell recording method [29]. Briefly, the Na^+-based bath solution consisted of (in mM) 120 NaCl, 5 KCl, 2 $CaCl_2$, 1 $MgCl_2$, 10 HEPES, and 10 D-glucose. (pH 7.4 adjusted by NaOH, and 300 mosmol/kg-H_2O adjusted by D-mannitol). The pipette solution for these recordings contained (in mM) 55 K_2SO_4, 20 KCl, 5 $MgCl_2$, 0.2 EGTA, and 5 HEPES (pH 7.4 adjusted by KOH, and 285 mosmol/kg-H_2O adjusted by D-mannitol). An Ag-AgCl pellet with a 3M KCl-agar bridge was used as the reference electrode.

RT-PCR and Quantitative real-time PCR

Total RNA was extracted from both differentiated and undifferentiated PC12 cells using the NucleoSpin® RNA Plus kit (Takara Bio, Shiga, Japan), following the manufacturer's instructions. RNA concentration and purity were assessed using a NanoDrop ND-1000 spectrophotometer (Thermo Fisher Scientific, Waltham, MA, USA). Reverse transcription was carried out using the ReverTra Ace® qPCR RT Master Mix with gDNA Remover (TOYOBO, Osaka, Japan) according to the manufacturer's protocol. Gene expression levels of 5-HT receptors and voltage-gated Ca^{2+} channels were analyzed by PCR using cDNA synthesized from the extracted RNA. Glyceraldehyde-3-phosphate dehydrogenase (Gapdh) was used as a positive internal control. PCR amplification was conducted with KOD-Plus-Neo polymerase (TOYOBO) under the following thermal cycling conditions: initial denaturation at 94°C for 2.5 min, followed by 24 cycles of denaturation at 94°C for 15 s, annealing at 57°C for 30 s, and extension at 68°C for 45 s. The sequences of gene-specific primers used are listed in Table 1. PCR products were separated and visualized via agarose gel electrophoresis. Expression of specific 5-HT receptor subtypes and voltage-gated Ca^{2+} channel isoforms was further evaluated by both conventional RT-PCR and quantitative real-time PCR (qRT-PCR). qRT-PCR and data analysis were performed using an ABI 7500 Real-Time PCR System (Applied Biosystems, Foster City, CA, USA). Amplifications were performed using KOD SYBR qPCR MIX (TOYOBO) according to the manufacturer's instructions, with annealing at 57°C in a 20-µL reaction volume containing 100 ng cDNA. Gene-specific primers were the same as those used in the PCR. mRNA expression levels were compared using the $\Delta\Delta C_T$ method.

Table 1. Primer sets used for RT-PCR/qPCR. Primer sequences are listed 5′→3′; amplicon size indicates the expected product length in base pairs (bp)

Gene (rat)	Forward primer(5′→3′)	Reverse primer(5′→3′)	Amplicon(bp)
HTR1A	CCAAAGAGCACCTTCCTCTG	GACTGAAAGCCATGTGCTGA	570
HTR1B	TCTCCTATGGAGGGATGCAC	TCTCCCATCTCATGGTCTCC	519
HTR1D	TCTGCTGAGCTCTGTCCTGA	GTCCAGAGCGATGACACAGA	529
HTR1F	TCATTGTGACTCGGAAGCTG	GTGGGATGTAGAAGGCTCCA	438
HTR2A	AGCTCTGTGCGATCTGGATT	ACGGCCATGATATTGGTGAT	604
HTR2B	TGGCAGTTTCATGCTCTTTG	GGAAACGTAGCCTACCCACA	475
HTR2C	ATCGCTGGACCGGTATGTAG	AGCCAATCCACACAAACACA	632
HTR3A	ACTCATCCTGAGTGGCTGCT	CCACGTCCACAAACTCATTG	451
HTR3B	TCCATTGGCCTATGTTGTGA	ACAGTGCCCAGAGAGAGCAT	599
HTR4	AAGGCTTTCCAAGAGCATGA	CATGGTTGACACAGGACTGG	442
HTR5A	TTCCACCGAGTACCACACAA	TGACGGACAGTGAACACCAT	578
HTR6	ATCAGTACCCCTCCCCAAAC	GAAGGCAGTCCAAAGCAGAC	534
HTR7	ACCTGCTGAGTGGCTTCCTA	GGTAAGGTGATGGAGGCAGA	517
$Ca_v3.1$	ACGGGACCTGAAGAAGTGCTAC	ATCGACTCTCCGGAAGTTCTGC	586
$Ca_v3.2$	ATCAATCCCACCATCATCCGCA	ACCTTGGCTTTCCTGTGCTGTA	579
$Ca_v3.3$	CAGCCTACAGACCACACTGGAA	TCTTCCTTTTGCTCGCAGCATC	587
Gapdh	CATGCCGCCTGGAGAAACCTGCCA	GGGCTCCCCAGGCCCCTCCTGT	429

Measurement of Intracellular $[Ca^{2+}]_i$ Changes

Intracellular cytosolic calcium concentration ($[Ca^{2+}]_i$) was measured at room temperature using fura-2, a ratiometric fluorescent Ca^{2+} indicator. PC12 cells cultured on glass coverslips were incubated in Tyrode's solution containing 5 μM fura-2 acetoxymethyl ester (fura-2/AM) for 30 min at 37°C. Following incubation, the coverslips were transferred to a perfusion chamber (0.3 mL volume) mounted on the stage of an inverted fluorescence microscope (IX-81, Olympus, Tokyo, Japan). Fura-2 fluorescence was alternately excited at 340 and 380 nm using a Polychrome IV monochromator system (Till Photonics, Martinsried, Germany) equipped with a xenon arc lamp. Emitted fluorescence was collected through a 475 nm long-pass emission filter and captured using a digitally cooled CCD camera (Hamamatsu Photonics, Shizuoka, Japan). Image acquisition was performed at 10-s intervals, and the fluorescence ratio (F340/F380) was calculated using MetaFluor software (Molecular Devices, San Jose, CA, USA). Changes in intracellular Ca^{2+} levels in response to receptor stimulation were expressed as ΔRatio values, calculated by subtracting the baseline ratio (averaged over the first min of recording) from the peak response induced by 50 μM 5-HT. Test compounds were applied 30 s prior to 5-HT stimulation. All experiments were conducted in Tyrode's solution.

Acetylcholine Release Assay in PC12 Cells

For acetylcholine (ACh) secretion assays, PC12 cells were seeded at 1.2×10^4 cells/well onto 96-well collagen-coated plates (Thermo Fisher Scientific, Waltham, MA, USA). Following differentiation induced by 50 ng/mL nerve growth factor (NGF) for 4 d, cells were gently washed twice with Tyrode's solution and incubated at 37 °C for 30 min to assess ACh release. The supernatants were then collected, and ACh concentrations were quantified using Amplex™ Acetylcholine/Acetylcholinesterase Assay Kit (Invitrogen), following the manufacturer's instructions.

Measurement of Intestinal Contractile Activity

Following cervical dislocation of adult rats, a midline abdominal incision was made immediately, and segments of the large intestine (colon and rectum) were excised. Luminal contents were flushed with ice-cold Krebs-Ringer solution saturated with 100% O_2. The cleaned intestinal segments were transferred to a Petri dish containing oxygenated, ice-cold Krebs-Ringer solution. The intestinal tissue was then cut into rings (12–15 mm in length) and mounted vertically in 5-mL organ baths filled with Krebs-Ringer solution maintained at 35°C and continuously bubbled with 100% O_2. Each ring was suspended between two stainless steel hooks: one fixed, and the other connected to an isometric force transducer (Type 45196A, NEC San-ei Instruments Co., Ltd., Tokyo, Japan). Contractile responses were recorded using a LabChart system (AD Instruments, Sydney, Australia) connected to a PowerLab data acquisition unit. A resting tension of 0.25–0.5 g was applied, and the tissues were allowed to equilibrate for 30 min before measurements began. After equilibration, spontaneous contractions were recorded. In separate experiments, tissues were pretreated with HST or specific antagonists for 10 min, followed by exposure to 5-HT (50 μM) for an additional 10 min to evaluate inhibitory effects. The Krebs-Ringer solution contained (in mM): 118 NaCl, 4.7 KCl, 2.5 $CaCl_2$, 1.2 $MgSO_4$, 1.2 KH_2PO_4, 4 $NaHCO_3$, 10 HEPES, and 11 glucose. The pH was adjusted to 7.4 by bubbling with 100% O_2. Contractile force was expressed as the maximum isometric tension (g/g wet tissue) in response to drug application. In organ bath experiments, n represents the number of individual tissue rings. Each ring was treated as an experimental unit, and multiple rings (up to 10) were obtained from a single animal. Tissues were collected from five rats. Rings from the same animal were distributed across different experimental groups, and experimental conditions were randomized across preparations to minimize potential bias. Blinding was not applied during data acquisition due to the nature of the experimental setup; however, data analysis was performed using predefined criteria. Data are presented as mean ± standard error of the mean (SEM). Statistical analysis was conducted using one-way ANOVA for dose-response comparisons and paired Student's t-tests for individual group comparisons. A p-value < 0.05 was considered statistically significant.

Statistical evaluation

All experimental data are presented as mean ± standard error of the mean (SEM), derived from at least three independent experiments for each condition. For cellular experiments, comparisons among multiple groups were performed using one-way ANOVA followed by Tukey's post hoc test. For two-group comparisons, Student's t-test was used. A p-value < 0.05 was considered statistically significant.

Results

Serotonin induces cell volume reduction in differentiated PC12 cells

Serotonin (5-HT) is a key mediator in neuronal signaling and has been implicated in the pathophysiology of irritable bowel syndrome (IBS) [7, 30]. Although Hange-shashin-to (HST) is clinically used for IBS, its cellular mechanisms remain unclear. To address this, the present study examined whether 5-HT induces cell volume changes in NGF-differentiated PC12 cells, a neuron-like model commonly used to study neuronal differentiation and neurotransmission. Secretory volume decrease (SVD) is a recognized indicator of neuronal activation and transmitter release [20]; therefore, 5-HT-evoked volume responses were assessed as an initial functional readout.

Initially, undifferentiated PC12 cells were examined to determine their responsiveness to 5-HT. Cross-sectional area (CSA), a proxy for cell volume, was measured over time following 5-HT application. In undifferentiated cells, 5-HT (50 μM), a concentration commonly used in electrophysiological studies of 5-HT receptors [10], did not produce a significant change in CSA (Fig. 1A,B; blue). In contrast, high-potassium (High K^+) solution, used as a positive control to induce membrane depolarization, produced a robust reduction in CSA (Fig. 1A–C; red), demonstrating that undifferentiated cells are capable of depolarization-induced volume decrease. Subsequently, NGF-differentiated PC12 cells, a neuron-like model, were evaluated. Application of 5-HT (50 μM) induced a significant, time-dependent decrease in CSA over 30 min (Fig. 1D,E; blue), consistent with activation of SVD. High K^+ similarly reduced CSA in differentiated cells (Fig. 1D–F; red), indicating that both 5-HT and depolarization trigger volume reduction in this differentiated neuronal phenotype.

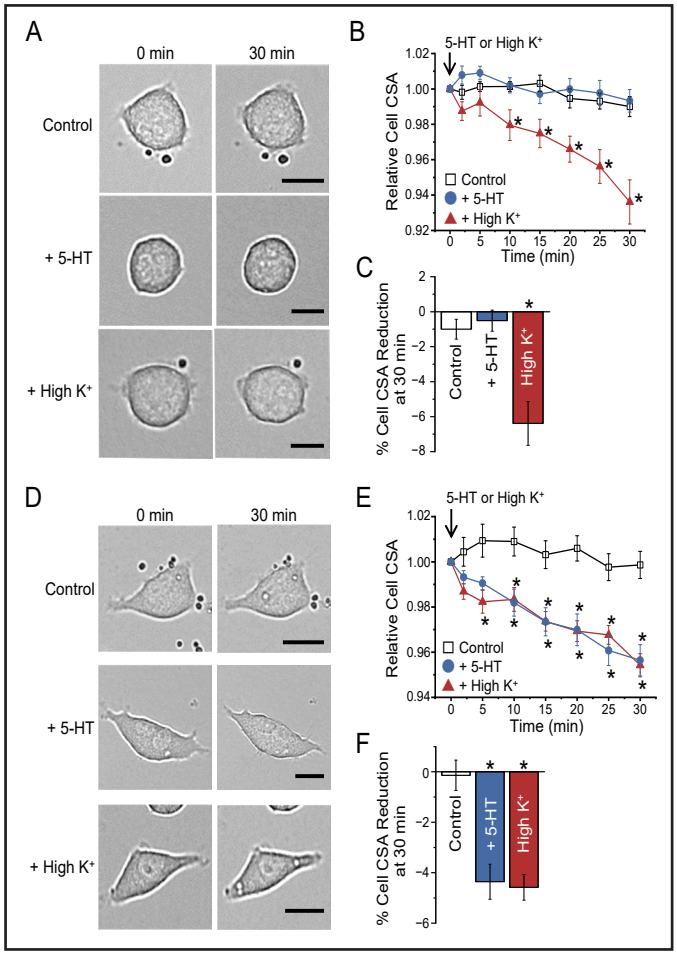

Fig. 1. Serotonin induces cell shrinkage in differentiated PC12 cells. (A, D) Representative light microscopy images of undifferentiated (A) and differentiated PC12 cells (D) at 0 and 30 min under control conditions and after application of serotonin (5-HT) or high-potassium (High K^+) solution. Scale bars indicate 50 μm. (B, E) Time course of changes in mean relative cell cross-sectional area (CSA) in undifferentiated (B) and differentiated PC12 cells (E). CSA values at each time point are normalized to those at 0 min (n = 12 cells for control, n = 15 cells for 5-HT, n = 13 cells for High K^+). (C, F) Percentage reduction of CSA after 30 min under control conditions and following application of 5-HT or High K^+ (n = 6 cells for control, n = 5 cells for 5-HT, n = 6 cells for High K^+). Data are presented as mean ± SEM. Statistical analysis: one-way ANOVA followed by Tukey's post hoc test. *p<0.05 versus control.

These results demonstrate that 5-HT induces cell volume reduction specifically in differentiated PC12 cells, suggesting that differentiation-dependent expression of serotonergic receptors is required for this response. Supplementary analyses further revealed that 5-HT-induced CSA reduction in differentiated PC12 cells was dependent on extracellular Ca^{2+} and was significantly attenuated by pharmacological inhibition of voltage-gated Ca^{2+} channels, including T-type channels (Fig. S2).

HST suppresses 5-HT-induced cell volume reduction in differentiated PC12 cells

We next investigated whether HST modulates 5-HT-induced cell volume reduction in differentiated PC12 cells. Co-application of HST with 5-HT significantly attenuated the time-dependent decrease in CSA normally induced by 5-HT (Fig. 2A; blue vs. purple). Quantification at 30 min confirmed a significant reduction of the 5-HT response by HST (Fig. 2B). To determine whether the inhibitory effect of HST is concentration-dependent, CSA reduction was measured across a range of HST concentrations. The resulting dose-response curve revealed a clear concentration-dependent suppression of 5-HT-induced volume reduction, with a fitted IC_{50} of 91.6 μg/mL and a Hill coefficient of 1.6 (Fig. 2C). In contrast, HST had no effect on CSA reduction induced by High K^+, a depolarizing stimulus (Fig. 2A, B, olive bars), indicating that HST has no general inhibitory effect on depolarization-induced volume changes.

These findings indicate that HST selectively suppresses 5-HT-mediated signaling pathways that underlie SVD, rather than interfering with downstream mechanisms shared with membrane depolarization.

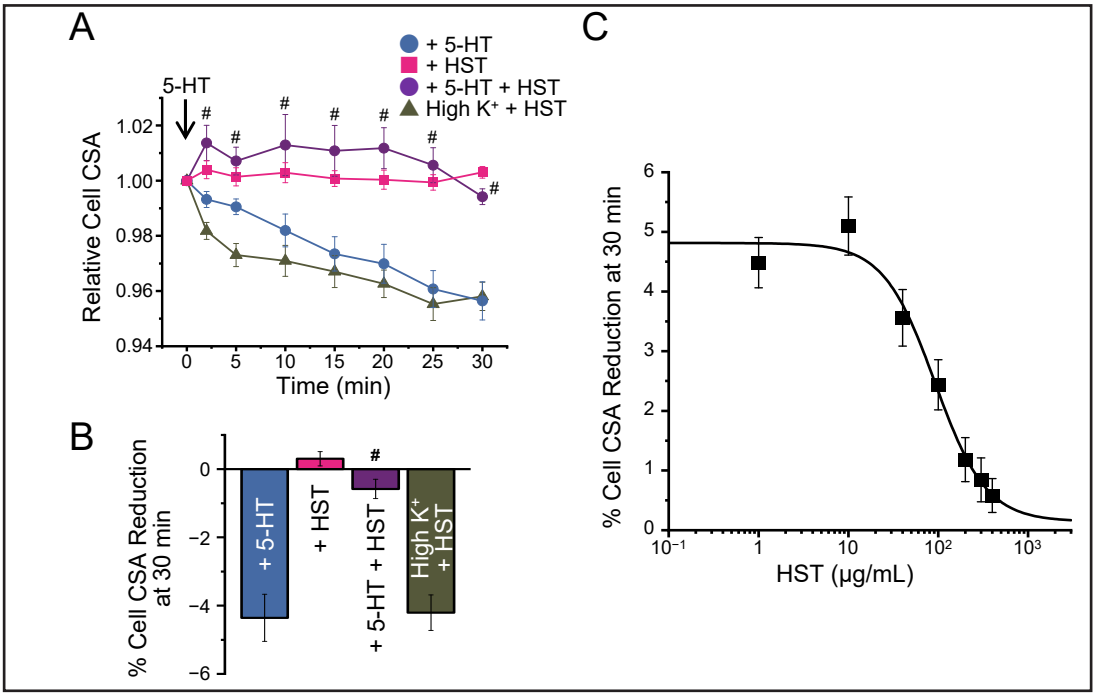

Fig. 2. HST attenuates serotonin-induced cell volume reduction in differentiated PC12 cells in a concentration-dependent manner. (A) The time course of changes in relative CSA in differentiated PC12 cells following application of 5-HT (50 μM) or High K^+ (80 mM) solution at time zero, in the presence or absence of HST (400 μg/mL). CSA values were normalized to those at 0 min (n = 9 cells for control, n = 10 cells for 5-HT, n = 10 cells for 5-HT + HST). (B) Quantification of CSA reduction at 30 min under each condition with or without HST treatment (n = 9-10 cells for each group). Statistical analysis: one-way ANOVA followed by Tukey's post hoc test. (C) Concentration-dependent inhibitory effect of HST on 5-HT-induced cell volume reduction. The data were fitted using the Hill equation, yielding an IC_{50} of 91.6 μg/mL and a Hill coefficient of 1.6 (n = 8, 9, 10, and 12 cells per concentration). Statistical analysis: nonlinear regression analysis. Data are presented as mean ± SEM. #p<0.05 versus 5-HT.

Expression of 5-HT receptor subtypes in differentiated PC12 cells and involvement of 5-HT3A receptors in cell volume reduction

The expression profile of 5-HT receptor mRNAs in differentiated PC12 cells was examined using RT-PCR to identify which subtypes are responsible for the observed 5-HT-induced cell volume reduction. Analysis of the 13 subtypes tested (*HTR1A*, *HTR1B*, *HTR1D*, *HTR1F*, *HTR2A*, *HTR2B*, *HTR2C*, *HTR3A*, *HTR3B*, *HTR4*, *HTR5A*, *HTR6*, *HTR7*) suggested that differentiation enhances 5-HT3A receptor mRNA in differentiated cells compared to undifferentiated cells (Fig. 3A, B).

To assess the functional involvement of this receptor subtype, we then pharmacologically inhibited 5-HT3A and 5-HT2B receptors using the selective antagonists ramosetron and RS-127445, respectively [31-33]. While ramosetron significantly suppressed the 5-HT-induced reduction in CSA, RS-127445 did not exhibit any notable effect (Fig. 3C, D). These results support the conclusion that the 5-HT-induced cell volume reduction in differentiated PC12 cells is predominantly mediated through 5-HT3A receptors.

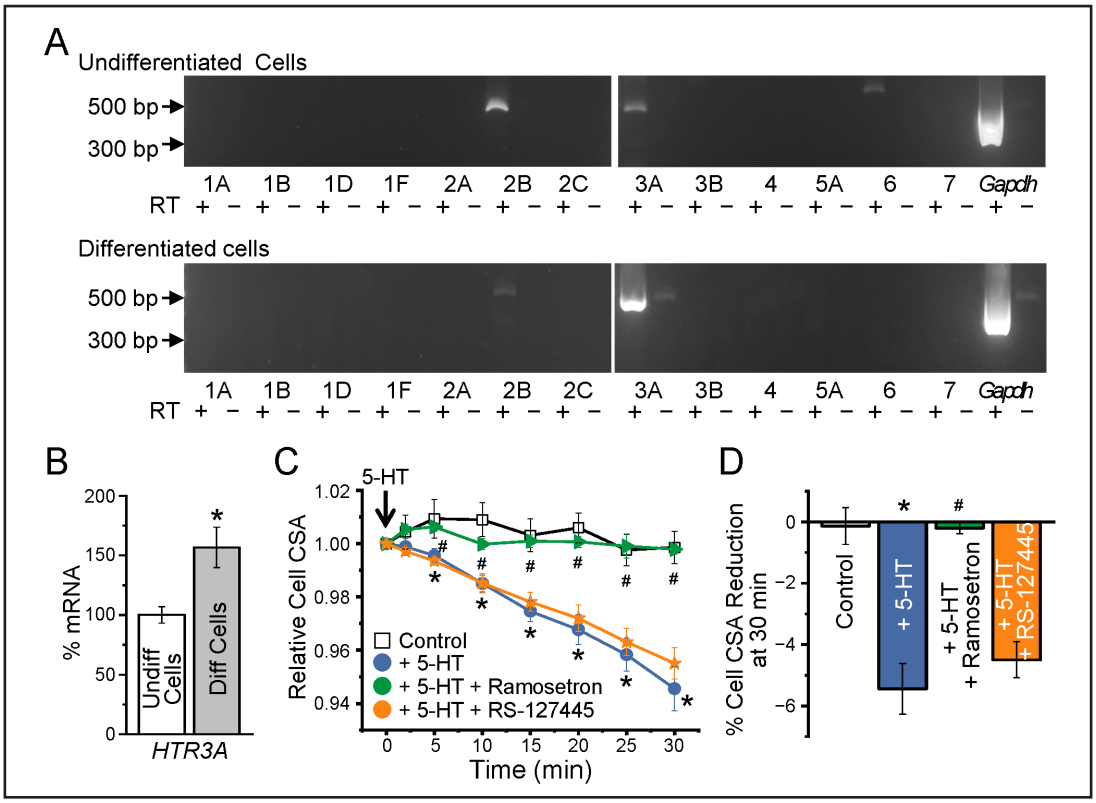

Fig. 3. Expression of 5-HT3A receptor in differentiated PC12 cells and its involvement in 5-HT-induced cell volume reduction. (A) Representative RT-PCR images showing mRNA expression of HTR (5-HT receptor) subtypes (HTR1A, HTR1B, HTR1D, HTR1F, HTR2A, HTR2B, HTR2C, HTR3A, HTR3B, HTR4, HTR5A, HTR6, and HTR7) in undifferentiated (top) and differentiated (bottom) PC12 cells. Gapdh was used as an internal control. RT(+) and RT(−) indicate the presence or absence of reverse transcriptase, respectively. (B) Quantitative real-time PCR analysis of HTR3A mRNA expression in undifferentiated and differentiated PC12 cells. Data are represented as mean ± SEM (N = 3 independent experiments), *p<0.05 versus undifferentiated cells. (C) Time course of changes in mean relative CSA in differentiated PC12 cells. CSA values at each time point are normalized to the 0 min value for each cell. 5-HT (50 μM), the selective 5-HT3 receptor antagonist ramosetron (10 μM, green symbols/line) or the selective 5-HT2 receptor antagonist RS-127445 (10 μM, orange symbols/line) were applied at 0 min, except in control conditions (n = 10 cells for control, n = 12 cells for 5-HT, n = 11 cells for ramosetron, n = 10 cells for RS-127445). (D) Percentage reduction of CSA after 30 min under control conditions and following treatment with 5-HT in the presence or absence of ramosetron or RS-127445. Data are presented as mean ± SEM (n = 8 cells for control, n = 10 cells for 5-HT, n = 12 cells for ramosetron, n = 11 cells for RS-127445; N = 5–6 independent experiments). Statistical analysis: one-way ANOVA followed by Tukey's test. *p<0.05 versus Control; #p<0.05 versus 5-HT.

HST inhibits 5-HT3A receptor-mediated cationic currents

To directly evaluate whether HST modulates 5-HT3A receptor activity, we investigated its effect on 5-HT-induced cationic currents in HEK293T cells heterologously expressing human 5-HT3A receptors. Whole-cell patch-clamp recordings at a holding potential of −70 mV revealed that application of 5-HT (50 μM) elicited robust inward cationic currents in 5-HT3A-expressing cells. The concentration of 5-HT (50 μM) was selected to robustly activate 5-HT3A receptor–mediated currents, enabling consistent evaluation of inhibitory effects under near-maximal stimulation conditions. In contrast, vector-transfected control cells (mock) exhibited no such currents (Fig. 4Aa, b, B), consistent with previous findings [34, 35].

Pre-treatment with either the selective 5-HT3 antagonist ramosetron (10 μM) or HST (400 μg/mL) significantly suppressed the 5-HT-induced currents (Fig. 4Ac, d, B). During pre-application, neither HST nor ramosetron alone induced detectable currents, and stable baseline recordings were confirmed for at least 1 min before subsequent 5-HT application (n = 5–8).

To further characterize the inhibitory mechanism, current–voltage (I–V) relationships were analyzed using ramp pulses from −100 to +100 mV. 5-HT evoked inward currents with a typical cationic profile, whereas HST reduced current amplitudes across a broad voltage range without significantly altering the reversal potential (Fig. 4C–E). These findings suggest that HST suppresses channel conductance rather than altering ion selectivity or voltage-dependent gating.

We next examined the effects of HST on voltage dependence by analyzing the conductance–voltage (G–V) relationship. Although overall conductance was reduced, normalization of conductance relative to values at −100 mV revealed no significant shift in voltage dependence (Fig. 4E–G), further supporting a voltage-independent inhibitory mechanism.

Kinetic analyses revealed that HST modulates channel gating dynamics. The activation phase, fitted with a single exponential function (inset in Fig. 4H), was significantly accelerated in the presence of HST. In contrast, desensitization kinetics, fitted with a double exponential function, showed a selective prolongation of the slow component of current decay (Fig. 4H–J). Quantitative analysis demonstrated that HST significantly shortened the activation time constant while increasing the contribution of the slow desensitization component, indicating preferential modulation of slower gating processes.

Taken together, these results demonstrate that HST inhibits 5-HT3A receptor–mediated cation currents through suppression of channel activity and modulation of gating kinetics, particularly desensitization. The lack of a shift in reversal potential or voltage dependence supports a mechanism consistent with non-competitive or allosteric inhibition rather than classical competitive antagonism.

HST suppresses 5-HT-induced depolarization, intracellular Ca^{2+} elevation, and acetylcholine release in differentiated PC12 cells

The physiological consequences of 5-HT3A receptor activation and the potential modulatory effects of HST were investigated by evaluating 5-HT-induced membrane depolarization, intracellular calcium ($[Ca^{2+}]_i$) elevation, and acetylcholine (ACh) secretion in differentiated PC12 cells.

Consistent with our electrophysiological recordings showing that 5-HT–evoked currents are detectable but relatively small in PC12 cells (Fig. 5A, B), yet consistently observed and pharmacologically sensitive, we next examined the downstream functional responses mediated by 5-HT3A receptor activation.

Membrane potential changes were measured using the nystatin-perforated whole-cell patch-clamp technique. After stabilization at a baseline membrane potential of −52.35 ± 1.3 mV (n = 24), application of 5-HT (50 μM) caused significant membrane depolarization. Pretreatment with HST (400 μg/mL) or the selective 5-HT3 receptor antagonist ramosetron

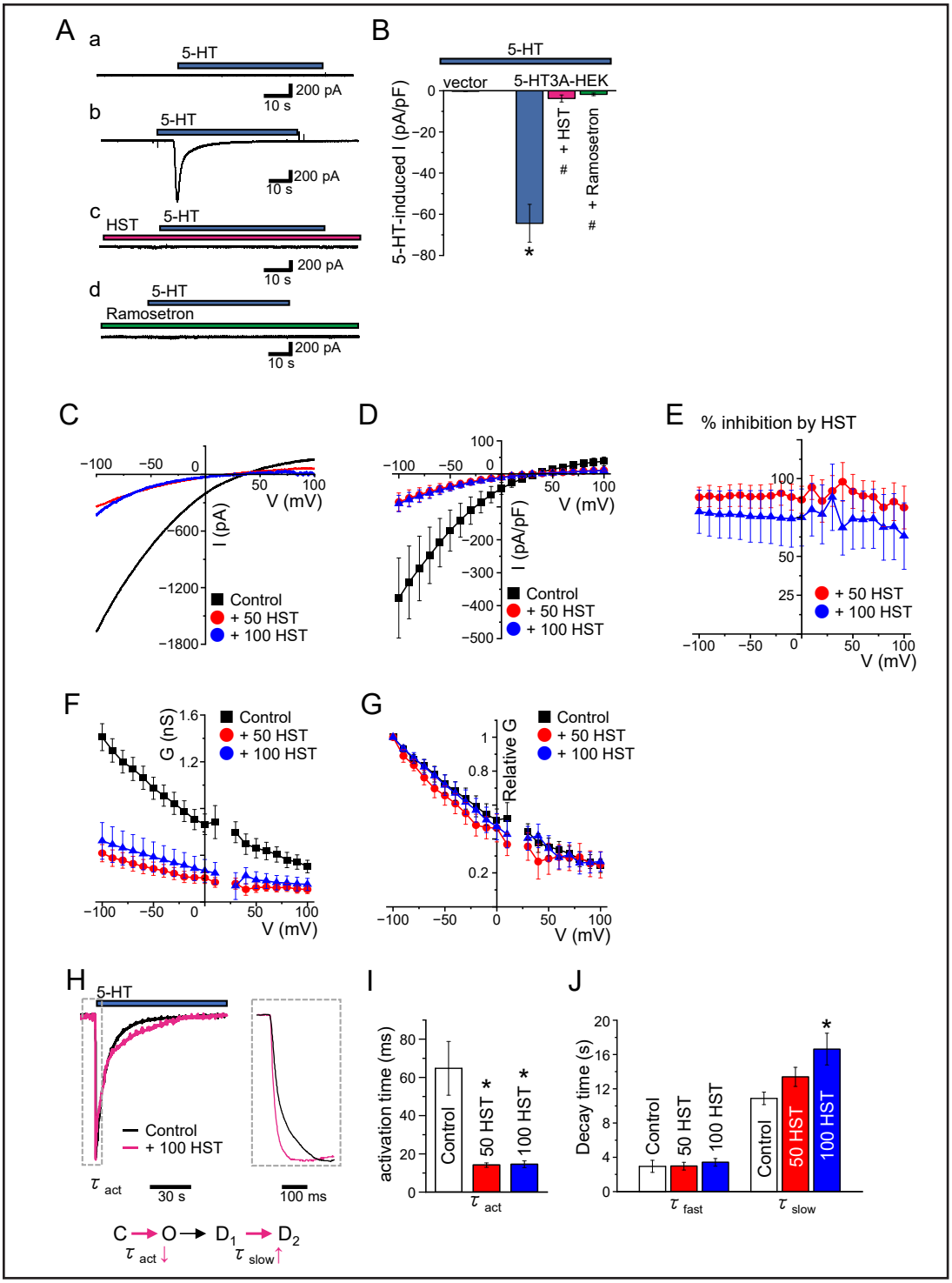

Fig. 4. Electrophysiological analysis of serotonin-induced cation currents in 5-HT3A-expressing HEK293T cells. (A) Representative whole-cell current traces recorded from HEK293T cells voltage-clamped at −70 mV. Traces are shown for cells transfected with an empty vector (mock) (a) or the human 5-HT3A receptor cDNA (5-HT3A) (b-d). 5-HT (50 μM, blue bars), HST (400 μg/mL, pink bars), and the selective 5-HT3 receptor antagonist ramosetron (10 μM, green bars) were applied as indicated. (B) Peak 5-HT-induced current density (pA/pF) was measured at −70 mV under the indicated conditions. (C, D) Current–voltage (I–V) relationships obtained using ramp pulses from −100 to +100 mV. HST (50 and 100 μg/mL) reduced current amplitudes across a broad voltage range without significantly altering the reversal potential. (E) Representative inhibition profile. (F-G) Voltage dependence of conductance (G-V relationship). (F) Absolute conductance. (G) Normalized conductance. (H) Representative current traces showing activation and desensitization kinetics. Insets show expanded traces used for fitting. (I, J) Quantitative analysis of kinetic parameters. Activation time constants (τ_{act}) were obtained by fitting with a single exponential function, and desensitization was fitted with a double exponential function (fast and slow components). HST significantly shortened τact and selectively prolonged the slow desensitization component (τ_{slow}). Data are presented as mean ± SEM (n = 5 cells for mock, n = 8 cells for 5-HT3A, n = 7 cells for HST, n = 6 cells for ramosetron). Statistical analysis: one-way ANOVA followed by Tukey's test. *p<0.05 versus mock, #p<0.05 versus 5-HT alone in 5-HT3A-expressing cells.

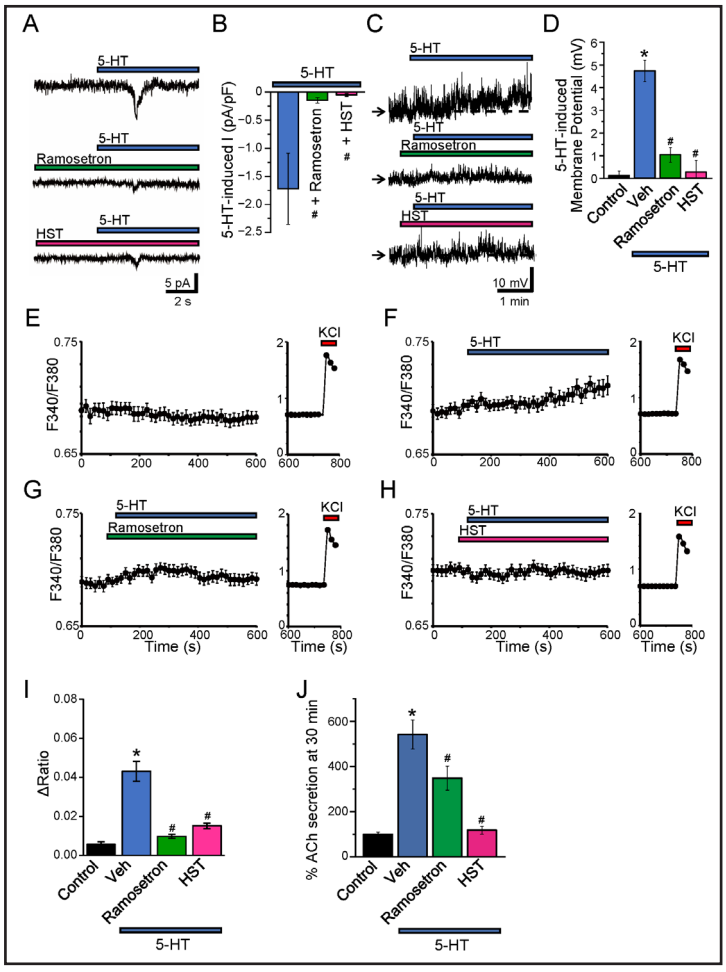

Fig. 5. Effects of HST on 5-HT-induced current, depolarization, intracellular Ca^{2+} responses, and acetylcholine release in differentiated PC12 cells. (A) Representative whole-cell current traces recorded from differentiated PC12 cells. 5-HT (50 μM, blue bar), HST (400 μg/mL, pink bar), and ramosetron (10 μM, green bar) were applied as indicated. (B) Quantification of peak current amplitudes under the indicated conditions. Data are presented as mean ± SEM (n = 8 cells for 5-HT, n = 8 cells for HST, n = 8 cells for ramosetron). (C) Representative recordings of membrane potential in differentiated PC12 cells measured using the nystatin-perforated patch clamp technique. 5-HT (50 μM, blue bar), HST (400 μg/mL, pink bar), and ramosetron (10 μM, green bar) were applied as indicated. The arrow indicates −50 mV. (D) Membrane potential changes were measured under the indicated conditions. Data are presented as mean ± SEM (n = 7 cells for control, n = 10 cells for 5-HT, n = 24 cells for HST, n = 18 cells for ramosetron). *p<0.05 versus Control, #p<0.05 versus 5-HT alone. (E–H) Representative time course intracellular Ca^{2+} response (F340/F380) in differentiated PC12 cells following application of 5-HT (50 μM) with or without pretreatment with HST or ramosetron, as indicated. At the end of each recording, High K^+ solution (KCl) was applied as a depolarizing positive control. (I) Quantification of peak intracellular Ca^{2+} responses (Δ ratio) under the indicated conditions. Data are presented as mean ± SEM (n = 21 cells for control, n = 30 cells for 5-HT, n = 44 cells for HST, n = 32 cells for ramosetron). *p<0.05 versus Control, #p<0.05 versus 5-HT alone. (J) Acetylcholine (ACh) release from differentiated PC12 cells following stimulation with 5-HT (50 μM), measured under the indicated conditions (n = 9 samples for control, n = 12 samples for 5-HT, n = 16 samples for ramosetron, n = 16 samples for HST). Data are mean ± SEM. Statistical analysis: one-way ANOVA followed by Tukey's test. *p<0.05 versus Control, #p<0.05 versus 5-HT alone (Veh).

(10 μM) significantly attenuated this effect (Fig. 5C, D), suggesting that HST reduces 5-HT3A receptor-mediated neuronal excitation.

We next measured $[Ca^{2+}]_i$ using fura-2 ratiometric fluorescence imaging. Application of 5-HT elicited a significant increase in $[Ca^{2+}]_i$, whereas pretreatment with HST or ramosetron markedly suppressed this Ca^{2+} elevation (Fig. 5E–H; left panels, I). In contrast, High K^+-induced depolarization increased $[Ca^{2+}]_i$ independently of treatment (Fig. 5E–H; right panels), demonstrating that HST selectively inhibits 5-HT-mediated Ca^{2+} influx rather than causing a general suppression of Ca^{2+} entry.

To evaluate functional relevance, ACh release was assessed using an enzyme-coupled Amplex Red-based fluorometric assay. 5-HT stimulation significantly enhanced ACh release, whereas co-application of HST or ramosetron significantly reduced this response (Fig. 5J).

Collectively, these findings indicate that HST inhibits 5-HT3A receptor-mediated depolarization in parasympathetic-like differentiated PC12 cells, thereby suppressing the subsequent downstream $[Ca^{2+}]_i$ increase and neurotransmitter secretion.

HST attenuates 5-HT-induced intestinal contractions via 5-HT3 receptor inhibition

To examine the physiological relevance of the cellular findings, we evaluated the effects of HST on 5-HT-induced intestinal contractility using isolated rat colonic rings mounted in a Magnus apparatus. Application of 5-HT (50 μM) elicited robust phasic contractions of the colon (Fig. 6A). In contrast, application of HST (400 μg/mL) or the selective 5-HT3 receptor antagonist ramosetron (10 μM) alone did not significantly alter basal contractile activity during the pre-application period, and stable baseline tension was confirmed prior to subsequent 5-HT stimulation (n = 6-16). Pretreatment with HST (400 μg/mL) significantly attenuated these contractile responses, indicating an inhibitory effect on 5-HT-induced intestinal motility (Fig. 6A, B). Notably, the selective 5-HT3 receptor antagonist ramosetron (10 μM) also significantly reduced 5-HT-induced contraction amplitudes to a comparable degree. These results support the conclusion that HST suppresses intestinal hypercontractility through inhibition of 5-HT3 receptor-mediated signaling, consistent with cellular evidence in PC12 and HEK293T models.

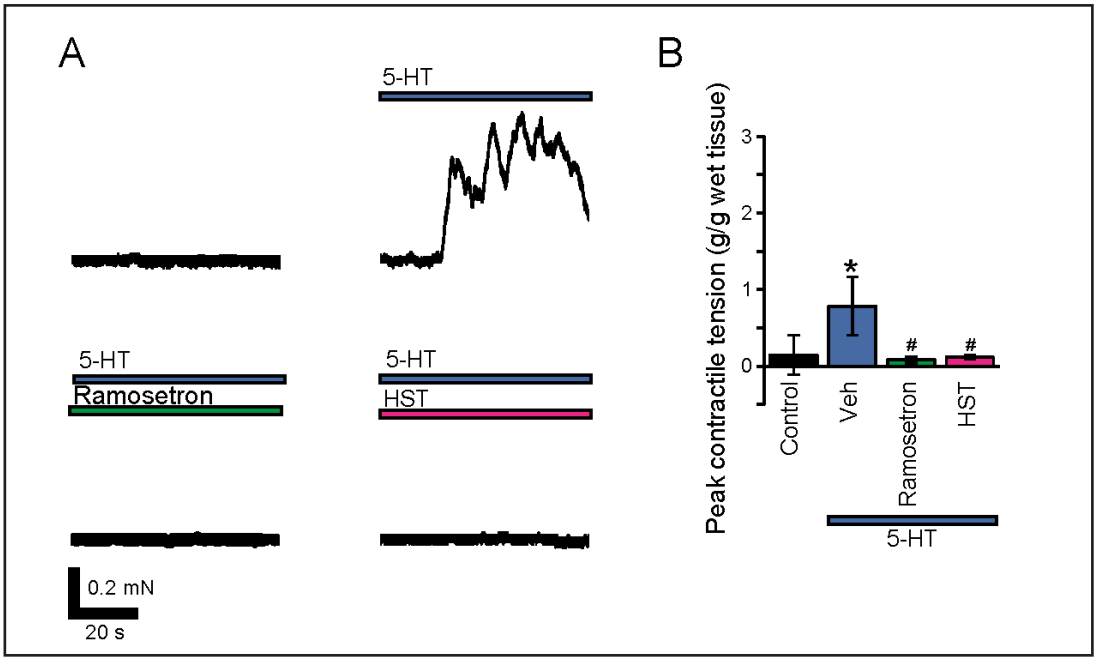

Fig. 6. Effects of HST on 5-HT-induced intestinal contractions. (A) Representative isometric tension recordings from rat colonic or rectal rings. 5-HT (50 μM) was applied alone or the 5-HT3 receptor antagonist ramosetron (10 μM) or following pretreatment with HST (400 μg/mL), as indicated. Contractile activity was recorded using the Magnus apparatus. (B) Peak contractile tension (g/g wet tissue) measured under the indicated conditions (n = 18 rings from 5 rats for control, n = 22 rings for 5-HT, n = 21 rings for ramosetron, n = 20 rings for HST). Statistical analysis: one-way ANOVA followed by Tukey's test. Data are presented as mean ± SEM. *p<0.05 versus Control, #p<0.05 versus 5-HT alone (Veh).

Discussion

In this study, we elucidated a previously unrecognized mechanism by which the Japanese medicine Hange-shashin-to (HST) exerts its therapeutic effect on diarrhea-predominant irritable bowel syndrome (IBS-D). Our findings indicate that HST attenuates serotonin (5-HT)-induced excitatory signaling in neuron-like cells. Using differentiated PC12 cells as a neuron-like model, we demonstrated that 5-HT induces a sustained decrease in cell volume, a characteristic response of secretory volume decrease (SVD) [20]. This cell volume reduction was observed only in differentiated cells (Fig. 1), suggesting that neuronal differentiation and associated receptor expression are prerequisites for the response.

Mechanistically, our findings indicate that the volume reduction is mediated by the 5-HT3A receptor subtype, a ligand-gated ion channel that promotes cation influx and subsequent membrane depolarization. RT-PCR and qRT-PCR analyses confirmed that 5-HT3A receptor mRNA expression was upregulated upon differentiation (Fig. 3A, B), and the 5-HT-induced CSA reduction was abolished by the selective 5-HT3 antagonist ramosetron (Fig. 3C, D). Furthermore, patch-clamp recordings in 5-HT3A-expressing HEK293T cells revealed that 5-HT evoked a strong inward current, which was inhibited by both ramosetron and HST, indicating direct receptor antagonism (Fig. 4A, B). While 5-HT3 receptor antagonists such as ramosetron have been clinically validated for IBS-D [36, 37], pharmacological modulation of this receptor by multi-component herbal formulations remains insufficiently characterized. Our findings provide electrophysiological evidence that HST inhibits 5-HT3A receptor-mediated cation currents. This inhibition does not involve changes in reversal potential or voltage dependence but rather reflects a reduction in channel conductance across a broad voltage range (Fig. 4). In addition, kinetic analysis revealed that HST accelerates activation while selectively prolonging the slow component of desensitization. These findings indicate that HST modulates channel gating dynamics, supporting a mechanism consistent with non-competitive or allosteric inhibition rather than classical competitive antagonism. Recent structural studies have further clarified the molecular architecture and gating mechanisms of the 5-HT3A receptor [38]. Given this receptor-level mechanism, it is important to consider how a multi-component formulation such as HST exerts its inhibitory effects.

HST is a multi-component formulation, and previous studies have identified several bioactive constituents, including [6]-shogaol, [6]-gingerol, baicalein, and berberine, which contribute to its pharmacological effects. Notably, combinations of these compounds have been shown to reproduce the activity of the whole formulation, supporting a multi-component and multi-target mechanism [39]. Although the present study demonstrates inhibitory effects of HST on 5-HT3A receptor–mediated signaling, the specific contribution of individual components remains to be clarified. It should be noted that the electrophysiological experiments in this study were performed using homomeric 5-HT3A receptors expressed in HEK293T cells. In native enteric neurons, 5-HT3 receptors form heteromeric assemblies with additional subunits such as 5-HT3C, 5-HT3D, and 5-HT3E, which exhibit distinct pharmacological and biophysical properties [40, 41] . Therefore, the present findings may not fully reflect the properties of native heteromeric receptors, and further studies will be required to evaluate the effects of HST in more physiologically relevant receptor systems. The reversibility of HST-mediated inhibition could not be conclusively determined in the present study. In our recording conditions, repeated 5-HT application caused pronounced desensitization, and current recovery remained markedly limited even after a 10-min washout period (29.65 ± 5.83% of control, n = 8 independent cells), suggesting a persistent or slowly reversible mode of inhibition, making it difficult to distinguish drug washout from agonist-induced desensitization. Therefore, further kinetic analyses will be required to clarify the reversibility and precise mode of inhibition. Consistent with this, our expression analysis indicated that HTR3A is the predominant subunit in differentiated PC12 cells, with minimal expression of the other 5-HT3 subunits (Fig. 3A, B). These limitations, including the use of a simplified neuronal model and lack of *in vivo* validation, should be considered when interpreting the present findings.

Despite these limitations, the functional relevance of HST was further supported by downstream physiological measurements. In differentiated PC12 cells, 5-HT caused whole-cell current (Fig. 5A, B), membrane depolarization (Fig. 5C, D), elevated intracellular Ca^{2+} levels (Fig. 5E-I), and enhanced acetylcholine (ACh) release (Fig. 5J), all of which were significantly attenuated by HST. In addition, supplementary analyses indicate that differentiation of PC12 cells is accompanied by increased expression of T-type Ca^{2+} channels ($Ca_V3.1$) and that 5-HT-induced CSA reduction is dependent on extracellular Ca^{2+} influx and is significantly attenuated by pharmacological inhibition of voltage-gated Ca^{2+} channels, including T-type channels (Fig. S2). Although the precise coupling between 5-HT3A receptor activation and Ca^{2+} entry pathways remains unclear, depolarization via 5-HT3A receptor-mediated cation influx may facilitate secondary activation of T-type Ca^{2+} channels, thereby amplifying Ca^{2+}-dependent responses. These findings suggest that HST inhibits excitatory neurotransmission via 5-HT3A receptors, possibly via direct receptor antagonism, suppressing Ca^{2+} influx and neurotransmitter release. Notably, high extracellular K^+ depolarization induced Ca^{2+} influx and decreased CSA even in the presence of HST (Fig. 1, 2, 5F), further supporting that HST specifically targets serotonergic signaling rather than a general depolarization mechanism. Further studies using fractionation approaches or individual compounds will be required to clarify the molecular basis of this activity.

Importantly, these cellular findings were validated in an ex vivo model of intestinal motility. 5-HT-induced contractions in isolated colonic tissue from rats were significantly attenuated by both HST and ramosetron (Fig. 6A, B). This indicates the physiological relevance of the *in vitro* results and supports the idea that HST regulates enteric neurotransmission and intestinal contractility via the 5-HT3A receptor pathway. The HST concentration used in this study (up to 400 μg/mL) reflects local intestinal exposure rather than systemic levels. Kampo medicines undergo metabolism by intestinal microbiota prior to absorption, resulting in low plasma but potentially high luminal and mucosal concentrations. For example, baicalin is converted to baicalein by intestinal bacteria [42], and its pharmacokinetics are strongly influenced by gut microbiota [43]. From a dosing perspective, a typical clinical dose of HST (approximately 2.5 g per administration) could theoretically yield luminal concentrations in the mg/mL range when distributed within gastrointestinal fluid volumes [44], supporting the physiological plausibility of the concentrations used in this study. This estimated luminal concentration exceeds the IC_{50} observed in our assays (~91.6 μg/mL) and the working concentration used in the present study (400 μg/mL), supporting their physiological plausibility as local intestinal exposure levels. However, the concentrations in deeper layers such as the myenteric plexus remain unclear and require further investigation. In addition to these pharmacokinetic considerations, previous pharmacological studies have reported that Hange-shashin-to does not significantly suppress 5-HT-induced diarrhea [45]. In that study, 5-HT was administered systemically via subcutaneous injection, which likely involves complex, multi-receptor, and systemic responses. In contrast, the present study specifically examines local 5-HT–induced responses, including 5-HT3A receptor–mediated ion channel activity and intestinal contraction (Figs. 4-6). Therefore, the apparent differences may reflect stimulus-specific and context-dependent effects, with HST selectively modulating 5-HT3-mediated signaling pathways.

In addition, a simplified neuronal model (differentiated PC12 cells) cannot fully recapitulate the complexity of the enteric nervous system, and further validation in *in vivo* models will be required to confirm the physiological and translational relevance of these findings. Hange-shashin-to is a clinically approved Kampo formulation in Japan, manufactured under standardized conditions with strict quality control to ensure batch-to-batch consistency. Although the active constituent(s) responsible for 5-HT3A receptor inhibition remain to be identified, the present study was designed to define the cellular and electrophysiological mechanisms of action of this standardized multi-component formulation. Moreover, HST is composed of multiple crude herbal components, and it remains unclear which specific constituents are responsible for the observed effects—an issue that will require future phytochemical and pharmacological dissection. The identification of

specific active components and their precise molecular targets remains an important area for future investigation.

Finally, beyond IBS-D, the 5-HT3A receptor is also implicated in other pathological states such as chemotherapy-induced nausea and vomiting (CINV), functional dyspepsia, and anxiety disorders [46, 47]. While these conditions share common 5-HT3-mediated pathways, the potential relevance of HST to these disorders remains speculative and was not addressed in the present study. Given its broad modulation of 5-HT3A receptor activity, HST or its active constituents may have therapeutic potential for these 5-HT-related conditions. Recent advances in IBS research highlight the importance of patient stratification and targeted therapeutic approaches based on underlying pathophysiological mechanisms, including serotonergic signaling. Recent clinical evidence further supports the therapeutic relevance of Hange-shashin-to (HST) in IBS-D. A multicenter retrospective study by Yoshida et al. (2025) demonstrated significant improvements in stool frequency, stool consistency, and abdominal pain following HST treatment, along with alterations in gut microbiota composition [14]. Although the present study focuses on receptor-level mechanisms, inhibition of 5-HT3A receptor–mediated signaling may contribute to these clinical effects by suppressing enteric excitatory neurotransmission and intestinal hypermotility. These findings suggest that multiple mechanisms, including both neuronal signaling and modulation of the microbiota, may underlie the clinical efficacy of HST.

Taken together, this study suggests that HST suppresses 5-HT-induced neuronal excitability and downstream motor responses by inhibiting cation conduction through the 5-HT3A receptor. These insights not only elucidate the molecular mechanisms underlying HST's efficacy in IBS-D but also provide mechanistic insights into its effects in IBS-D and support further investigation of serotonergic signaling in the gut–brain axis.

Conclusion

The present study demonstrates that HST suppresses 5-HT-induced neuronal excitation through inhibition of 5-HT3A receptor-mediated cation channel activity. This inhibition attenuates membrane depolarization, intracellular Ca^{2+} signaling, acetylcholine release, and downstream intestinal contractility, providing a mechanistic basis for the pharmacological actions of HST in 5-HT-mediated gastrointestinal dysfunction. These findings identify the 5-HT3A receptor as a molecular target of HST and provide new insight into the cellular mechanisms underlying the therapeutic effects of this clinically used Kampo medicine.

Acknowledgements

We are grateful to the members of our laboratory for their technical support and for providing the experimental setup and research environment essential for this study. We also thank Keitatsu Ishikawa for assistance with preliminary experiments.

Author Contributions

K.S-N. conducted all experiments and analysis. K.S-N., R.T., A.S., T.N. contributed to the investigation, writing, reviewing, editing, and validation of the findings. T.N. conceived and designed the work and wrote the manuscript.

Funding Source

This work was supported in part by Akita University Funding for Grant-in-Aid for Scientific Research (Re-challenge Promotion Expenses) (K.S-N. and T.N.), a grant from the Japan Kampo Medicine Education Foundation (grant number 2023; T.N.), JKA and its promotion funds from KEIRIN RACE (T.N.), and Kobayashi Foundation (T.N.).

Disclosure of AI Assistance

The authors used ChatGPT (OpenAI) to assist with English language editing and improvement of manuscript readability during manuscript preparation. All scientific content, data analyses, interpretation of the results, and conclusions were developed, verified, and approved by the authors.

Data Availability Statements

The datasets generated and/or analyzed during the current study are available from the corresponding author upon reasonable request.

Disclosure Statement

The authors declare no competing interests.

References

1 Casado-Bedmar M, Keita ÅV: Potential neuro-immune therapeutic targets in irritable bowel syndrome. Therap Adv Gastroenterol 2020;13:1756284820910630.
2 Quigley EMM: The Gut-Brain Axis and the Microbiome: Clues to Pathophysiology and Opportunities for Novel Management Strategies in Irritable Bowel Syndrome (IBS). J Clin Med 2018;7(1):6.
3 Tait C, Sayuk GS: The Brain-Gut-Microbiotal Axis: A framework for understanding functional GI illness and their therapeutic interventions. Eur J Intern Med 2021;84:1-9.
4 Crowell MD: Role of serotonin in the pathophysiology of the irritable bowel syndrome. Br J Pharmacol 2004;141:1285-1293.
5 Sikander A, Rana SV, Prasad KK: Role of serotonin in gastrointestinal motility and irritable bowel syndrome. Clin Chim Acta 2009;403:47-55.
6 Gershon MD, Tack J: The serotonin signaling system: from basic understanding to drug development for functional GI disorders. Gastroenterology 2007;132:397-414.
7 Gershon MD: Review article: serotonin receptors and transporters — roles in normal and abnormal gastrointestinal motility. Alimentary Pharmacology & Therapeutics 2004;20:3-14.
8 Kato S: Role of serotonin 5-HT_3 receptors in intestinal inflammation. Biol Pharm Bull 2013;36:1406-1409.
9 Zheng Y, Yu T, Tang Y, Xiong W, Shen X, Jiang L, Lin L: Efficacy and safety of 5-hydroxytryptamine 3 receptor antagonists in irritable bowel syndrome: A systematic review and meta-analysis of randomized controlled trials. PLoS One 2017;12:e0172846.
10 Thompson AJ, Lummis SC: The 5-HT3 receptor as a therapeutic target. Expert Opin Ther Targets 2007;11:527-540.
11 Kanehisa M, Goto S: KEGG: kyoto encyclopedia of genes and genomes. Nucleic Acids Res 2000;28:27-30.
12 Hitomi S, Ono K, Terawaki K, Matsumoto C, Mizuno K, Yamaguchi K, Imai R, Omiya Y, Hattori T, Kase Y, Inenaga K: [6]-gingerol and [6]-shogaol, active ingredients of the traditional Japanese medicine hangeshashinto, relief oral ulcerative mucositis-induced pain via action on Na+ channels. Pharmacological Research 2017;117:288-302.
13 He Y, Wu L, Qi X, Wang X, He B, Zhang W, Zhao W, Deng M, Xiong X, Wang Y, Liang S: Efficiency of Protective Interventions on Irinotecan-Induced Diarrhea: A Systematic Review and Meta-Analysis. Integr Cancer Ther 2024;23:15347354241242110.
14 Yoshida N, Yasuda T, Inagaki Y, Hasegawa D, Fukumoto K, Murakami T, Hirose R, Dohi O, Uchiyama K, Takagi T, Itoh Y: The Impact of Hangeshashinto on Symptoms and Gut Microbiota in Diarrhea-type Irritable Bowel Syndrome: A Retrospective Analysis. J Anus Rectum Colon 2025;9:105-116.
15 Lang F, Shumilina E, Ritter M, Gulbins E, Vereninov A, Huber SM: Ion channels and cell volume in regulation of cell proliferation and apoptotic cell death. Contrib Nephrol 2006;152:142-160.
16 Hoffmann EK, Lambert IH, Pedersen SF: Physiology of cell volume regulation in vertebrates. Physiol Rev 2009;89:193-277.
17 Wilson CS, Mongin AA: Cell Volume Control in Healthy Brain and Neuropathologies. Curr Top Membr 2018;81:385-455.

18 Bortner CD, Cidlowski JA: Ions, the Movement of Water and the Apoptotic Volume Decrease. Front Cell Dev Biol 2020;8:611211.
19 Okada Y, Shimizu T, Maeno E, Tanabe S, Wang X, Takahashi N: Volume-sensitive chloride channels involved in apoptotic volume decrease and cell death. J Membr Biol 2006;209:21-29.
20 Sato-Numata K, Numata T, Ueta Y, Okada Y: Vasopressin Neurons Respond to Hyperosmotic Stimulation with Regulatory Volume Increase and Secretory Volume Decrease by Activating Ion Transporters and Ca(2+) Channels. Cell Physiol Biochem 2021;55:119-134.
21 Itoh M, Yasunishi A, Imamura K, Kanamori-Katayama M, Suzuki H, Suzuki M, Carninci P, Kawai J, Hayashizaki Y: Constructing ORFeome resources with removable termination codons. Biotechniques 2006;41:44, 46, 48 passim.
22 Kimura K, Wakamatsu A, Suzuki Y, Ota T, Nishikawa T, Yamashita R, Yamamoto J, Sekine M, Tsuritani K, Wakaguri H, Ishii S, Sugiyama T, Saito K, Isono Y, Irie R, Kushida N, Yoneyama T, Otsuka R, Kanda K, Yokoi T, et al.: Diversification of transcriptional modulation: large-scale identification and characterization of putative alternative promoters of human genes. Genome Res 2006;16:55-65.
23 Ota T, Suzuki Y, Nishikawa T, Otsuki T, Sugiyama T, Irie R, Wakamatsu A, Hayashi K, Sato H, Nagai K, Kimura K, Makita H, Sekine M, Obayashi M, Nishi T, Shibahara T, Tanaka T, Ishii S, Yamamoto J, Saito K, et al.: Complete sequencing and characterization of 21,243 full-length human cDNAs. Nat Genet 2004;36:40-45.
24 Otsuki T, Ota T, Nishikawa T, Hayashi K, Suzuki Y, Yamamoto J, Wakamatsu A, Kimura K, Sakamoto K, Hatano N, Kawai Y, Ishii S, Saito K, Kojima S, Sugiyama T, Ono T, Okano K, Yoshikawa Y, Aotsuka S, Sasaki N, et al.: Signal sequence and keyword trap in silico for selection of full-length human cDNAs encoding secretion or membrane proteins from oligo-capped cDNA libraries. DNA Res 2005;12:117-126.
25 TSUMURA: Hange-shashin-to (TJ-14) Interview Form.
26 Sawada R, Iwata M, Umezaki M, Usui Y, Kobayashi T, Kubono T, Hayashi S, Kadowaki M, Yamanishi Y: KampoDB, database of predicted targets and functional annotations of natural medicines. Scientific Reports 2018;8:11216.
27 Schneider CA, Rasband WS, Eliceiri KW: NIH Image to ImageJ: 25 years of image analysis. Nature Methods 2012;9:671-675.
28 Sato K, Numata T, Saito T, Ueta Y, Okada Y: V_2 receptor-mediated autocrine role of somatodendritic release of AVP in rat vasopressin neurons under hypo-osmotic conditions. Sci Signal 2011;4:ra5.
29 Numata T, Fukuda R, Hirano M, Yamaguchi K, Sato-Numata K, Imahori H, Murakami T: Elucidation of the Mechanisms for the Underlying Depolarization and Reversibility by Photoactive Molecule. Cell Physiol Biochem 2020;54:899-916.
30 Fidalgo S, Ivanov DK, Wood SH: Serotonin: from top to bottom. Biogerontology 2013;14:21-45.
31 Bonhaus DW, Flippin LA, Greenhouse RJ, Jaime S, Rocha C, Dawson M, Van Natta K, Chang LK, Pulido-Rios T, Webber A, Leung E, Eglen RM, Martin GR: RS-127445: a selective, high affinity, orally bioavailable 5-HT2B receptor antagonist. Br J Pharmacol 1999;127:1075-1082.
32 Matsueda K, Harasawa S, Hongo M, Hiwatashi N, Sasaki D: A phase II trial of the novel serotonin type 3 receptor antagonist ramosetron in Japanese male and female patients with diarrhea-predominant irritable bowel syndrome. Digestion 2008;77:225-235.
33 Miyata K, Kamato T, Nishida A, Ito H, Katsuyama Y, Iwai A, Yuki H, Yamano M, Tsutsumi R, Ohta M, et al.: Pharmacologic profile of (R)-5-[(1-methyl-3-indolyl)carbonyl]-4,5,6,7-tetrahydro-1H- benzimidazole hydrochloride (YM060), a potent and selective 5-hydroxytryptamine3 receptor antagonist, and its enantiomer in the isolated tissue. J Pharmacol Exp Ther 1991;259:15-21.
34 Kaneez FS, White M: Patch Clamp Study of Serotonin-Gated Currents via 5-HT Type 3 Receptors by Using a Novel Approach SHAM for Receptor Channel Scanning. J Biomed Biotechnol 2004;2004:10-15.
35 Mott DD, Erreger K, Banke TG, Traynelis SF: Open probability of homomeric murine 5-HT3A serotonin receptors depends on subunit occupancy. J Physiol 2001;535:427-443.
36 Fukudo S, Matsueda K, Haruma K, Ida M, Hayase H, Akiho H, Nakashima Y, Hongo M: Optimal dose of ramosetron in female patients with irritable bowel syndrome with diarrhea: A randomized, placebo-controlled phase II study. Neurogastroenterol Motil 2017;29:e13023.
37 Min YW, Rhee PL: The clinical potential of ramosetron in the treatment of irritable bowel syndrome with diarrhea (IBS-D). Therap Adv Gastroenterol 2015;8:136-142.
38 Basak S, Gicheru Y, Rao S, Sansom MSP, Chakrapani S: Cryo-EM reveals two distinct serotonin-bound conformations of full-length 5-HT(3A) receptor. Nature 2018;563:270-274.

39 Kono T, Kaneko A, Matsumoto C, Miyagi C, Ohbuchi K, Mizuhara Y, Miyano K, Uezono Y: Multitargeted Effects of Hangeshashinto for Treatment of Chemotherapy-Induced Oral Mucositis on Inducible Prostaglandin E2 Production in Human Oral Keratinocytes. Integrative Cancer Therapies 2014;13:435-445.
40 Davies PA, Pistis M, Hanna MC, Peters JA, Lambert JJ, Hales TG, Kirkness EF: The 5-HT3B subunit is a major determinant of serotonin-receptor function. Nature 1999;397:359-363.
41 Kapeller J, Möller D, Lasitschka F, Autschbach F, Hovius R, Rappold G, Brüss M, Gershon MD, Niesler B: Serotonin receptor diversity in the human colon: Expression of serotonin type 3 receptor subunits 5-HT3C, 5-HT3D, and 5-HT3E. J Comp Neurol 2011;519:420-432.
42 Akao T, Kawabata K, Yanagisawa E, Ishihara K, Mizuhara Y, Wakui Y, Sakashita Y, Kobashi K: Baicalin, the Predominant Flavone Glucuronide of Scutellariae Radix, is Absorbed from the Rat Gastrointestinal Tract as the Aglycone and Restored to its Original Form. Journal of Pharmacy and Pharmacology 2000;52:1563-1568.
43 Kang MJ, Ko GS, Oh DG, Kim JS, Noh K, Kang W, Yoon WK, Kim HC, Jeong HG, Jeong TC: Role of metabolism by intestinal microbiota in pharmacokinetics of oral baicalin. Arch Pharm Res 2014;37:371-378.
44 Mudie DM, Amidon GL, Amidon GE: Physiological parameters for oral delivery and *in vitro* testing. Mol Pharm 2010;7:1388-1405.
45 Kase Y, Hayakawa T, Takeda S, Ishige A, Aburada M, Okada M: Pharmacological studies on antidiarrheal effects of Hange-shashin-to. Biol Pharm Bull 1996;19:1367-1370.
46 Faerber L, Drechsler S, Ladenburger S, Gschaidmeier H, Fischer W: The neuronal 5-HT3 receptor network after 20 years of research: evolving concepts in management of pain and inflammation. Eur J Pharmacol 2007;560:1-8.
47 Juza R, Vlcek P, Mezeiova E, Musilek K, Soukup O, Korabecny J: Recent advances with 5-HT(3) modulators for neuropsychiatric and gastrointestinal disorders. Med Res Rev 2020;40:1593-1678.